Electrochimica Acta 391 (2021) 138947

Contents lists available at ScienceDirect

Electrochimica Acta

journal homepage: www.elsevier.com/locate/electacta

On the behavior of CTAB/CTAOH adlayers on gold single crystal surfaces

José M. Gisbert-González, María V. Oliver-Pardo, Francisco J. Sarabia, Víctor Climent, Juan M. Feliu, Enrique Herrero*

Instituto de Electroquímica, Universidad de Alicante, Apdo. 99, E-03080 Alicante, Spain

ARTICLE INFO

Article history:
Received 11 June 2021
Revised 13 July 2021
Accepted 18 July 2021
Available online 26 July 2021

Keywords:
Gold
Single crystal electrodes
CTAB
CTAOH
Adsorption behavior

ABSTRACT

The behavior of adsorbed CTAB and CTAOH on gold single crystal electrodes has been studied in solutions with different pH values. For the different single crystal electrodes, the adsorbed adlayer formed by CTA^+ cations is in contact with the surface when the electrode charge is negative. As the surface charge becomes positive, the adlayer detaches from the surface and water molecules permeate through it, giving rise to characteristic peaks in the voltammogram. Charge and laser-induced jump temperature measurements show that the composition of the adlayer contains not only the CTA^+ cations but also anions, which are required to stabilize the adlayer. In alkaline solutions, the higher solubility of CTAB/CTAOH in alkaline solutions leads to the partial desorption of the adlayer when these species are not present in the solution. When CTAB or CTAOH are dissolved in the alkaline cell solution, the adlayer is strongly bonded to the surface in the whole potential window due to the negative charge of the surface.

1. Introduction

The adsorption of organic molecules on metallic surfaces is a subject of paramount importance because of its wide implications in multiple applications. Historically, the initial electrochemical studies were devoted to understanding the adsorption phenomenon and its applications to prevent corrosion [1]. However, the significance of this field goes far beyond that intended in those initial studies, and a myriad of applications are emerging nowadays in multiple fields such as the design of biomimetic systems and molecular nanoelectronics. The presence of adsorbed organic molecules on a metal modifies its properties. Thus, it has been used to tune the electronic properties of the substrate materials [2], to immobilize other molecules on the adlayer to build sensors [3], to form biomimetic membranes to study membrane processes [4], or in the synthesis of nanoparticles with special properties, because they act as surfactants and direct the growth of the nanoparticles [5].

In this context, cetyltrimethylammonium bromide (CTAB) has been widely used as a surfactant in the growth of metallic nanoparticles [6-8]. CTAB can be considered as a salt with a bromide anion and quaternary ammonium cation (CTA^+). This CTA^+ cation consists of three methyl groups and a hexadecyl group bonded to the nitrogen atom. Thus, the cation contains a polar hydrophilic head around the positively charged nitrogen atom and a hydrophobic tail (the hexadecyl group), giving rise to its surfactant properties. When used in the growth of nanoparticles, the synthetic procedure generally involves the creation of an initial seed, followed by one or several growth steps. Thus, their final shape depends on the exact conditions of the synthesis [7], where the concentration of surfactant, the ionic strength, and the specific chemical nature of the anions present in it are key parameters, stressing the importance of the adsorption behavior of this species on the surface in directing the growth [8-15].

Once the CTAB has been used for the synthesis of the nanoparticles, it has to be eliminated from the metallic surface, where it remains adsorbed, because it modifies the properties of the nanoparticles. This is especially important if the nanoparticles are to be used in biomedical applications because of the toxicity of this molecule. In fact, CTAB has antibacterial properties because it can permeate cellular membranes and interact with the cell DNA [16]. Thus experiments have been carried out to replace it from gold nanoparticles with other molecules [17]. CTAB forms a bilayer structure on gold nanorods, where the polar heads of the cations

* Corresponding author.
E-mail address: herrero@ua.es (E. Herrero).

https://doi.org/10.1016/j.electacta.2021.138947

are in contact with the gold surface and the tails are directed to the solution [18-20]. The hydrophobic nature of the tails drives the adsorption of the second layer of CTA^+ cations by the direct interaction of the tails. In the formation of the bilayer, the anion is also involved [13-15].

All these previous results highlight the importance of studying the adsorption behavior of CTA^+ layers on gold. As in any other chemisorption process, the surface structure of the substrate will have a significant influence on the interactions between the adsorbing molecule and the surface. For these reasons, the use of single-crystal electrodes is an excellent tool to simplify the experimental response and thus, to understand these processes. Previous results with the Au(111) surface have shown that CTA^+ cations form a stable layer in perchloric acid solutions [21]. Despite this stability, the distance between the adlayer and the electrode surface is modulated by the surface charge; when the electrode charge is negative, the adlayer is in direct contact with the surface. As the charge is made positive, the adlayer detaches from the surface due to coulostatic repulsion. In this work, additional insights into the behavior of the CTA^+ adlayers are obtained, highlighting the role of the pH, counteranion, and surface structure in this process. For this, the adsorption behavior of CTAB will be studied voltammetrically on gold basal planes and its behavior will be compared with that of CTAOH. The laser-induced temperature jump method will also be used to gain insight into the role of the anions in the stabilization of the adlayer.

2. Experimental

Gold single crystal electrodes were fabricated according to a modification of Clavilier's method [22,23]. For this, a 0.5 mm gold wire was melted, and a single crystal bead was formed after a slow cooling down procedure. The single crystal bead was then mounted in a four-cycle goniometer for its orientation and was cut according to the desired orientation with emery paper and polished until mirror finishing with diamond paste. Prior to any electrochemical experiment, the electrode was annealed in a propane/oxygen flame to burn and remove any organics that may have been adsorbed on the surface and to restore the surface order.

The solubility of CTAB is very low in acidic solutions and for this reason, the adlayers were formed at open circuit in an aqueous solution of CTAB or CTAOH. Since CTAB/CTAOH can form micelles when the concentration is above 1 mM, concentrations below and above this critical value were tested. Once the adlayer has been formed, the electrode is rinsed with water and transferred to the electrochemical cell, in which the electrode is immersed at 0.1 V.

Electrochemical experiments were carried out in a glass cell with a reversible hydrogen electrode (RHE) as reference and a gold counterelectrode. Supporting electrolyte solutions were prepared using concentrated perchloric acid (Merck Suprapur®), NaOH (Merck Suprapur®), and ultrapure water (18.2 MΩ cm, Elga Vivendi). CTAB/CTAOH solutions were prepared using CTAB, (BioUltra, for molecular biology, ≥ 99.0%, Sigma-Aldrich) and CTAOH (10 wt. % in H_2O, Sigma-Aldrich). All solutions were deoxygenated with Ar (N50, Air Liquide). Voltammetric experiments were carried out at room temperature using a wave signal generator (EG&G PARC 175), potentiostat (eDAQ 161), and digital recorder (eDAQ e-corder 401) workstation. Cyclic voltammograms were recorded at 50 mV s^{-1}.

2.1. Laser-induced jump temperature method

The laser-induced temperature jump method (litjm) has been used to obtain data regarding the water orientation at the interphase from which the magnitude of the interfacial electric field can be inferred. The details of this method are given elsewhere [24,25]. For these experiments, an additional electrode is required to be used as reference to measure the laser-induced potential change. In this case, a gold electrode was used, which was polarized at the same potential as the working electrode. The pulsed laser is used to raise the temperature of the working electrode, and the relaxation of the open circuit potential after this perturbation is measured. For this, the circuit between the working and reference electrodes is opened 200 µs before the laser pulse, and the change of the potential (ΔE) with respect to the fourth electrode is measured vs. time under constant charge conditions.

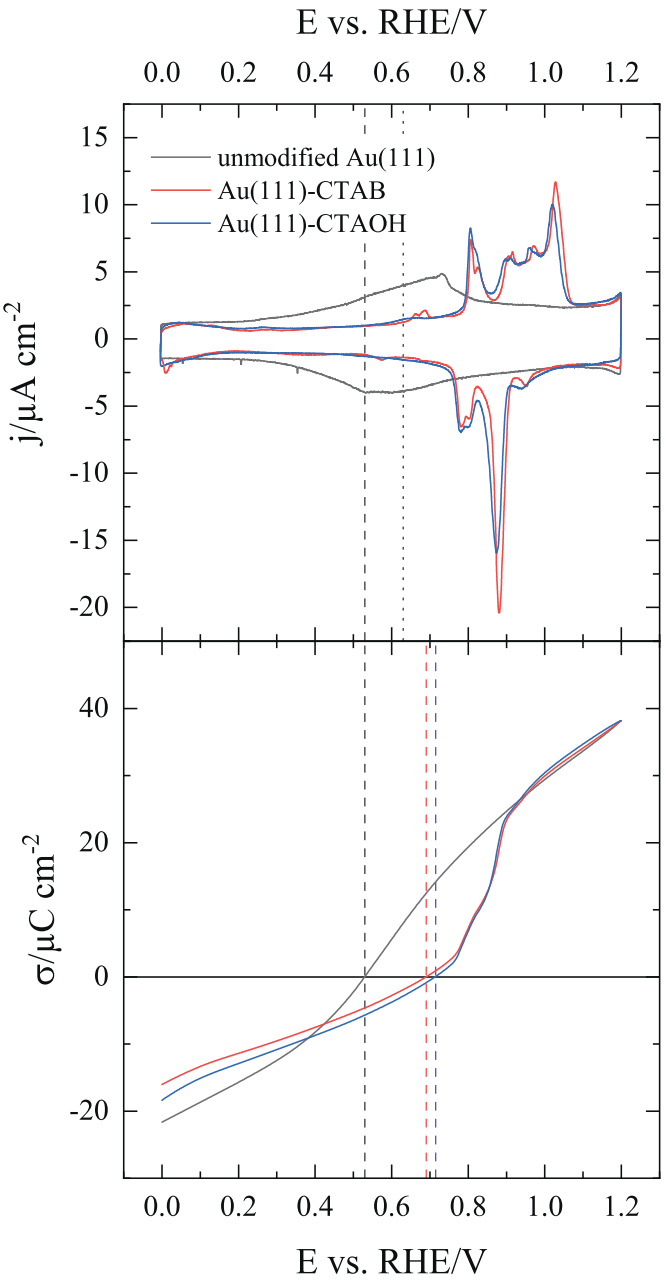

Figure 1. A) Stable voltammetric profiles for the unmodified Au(111) electrode and the CTAB and CTAOH modified Au(111) electrodes in 0.1 M $HClO_4$. The vertical lines mark the position of the pzc_u (dashed line) and pzc_r (dotted line) of the unmodified Au(111) surface. B) Charge curves obtained from the integration of the voltammetric profiles. The vertical lines reflect the point at which the curves cross the zero charge value.

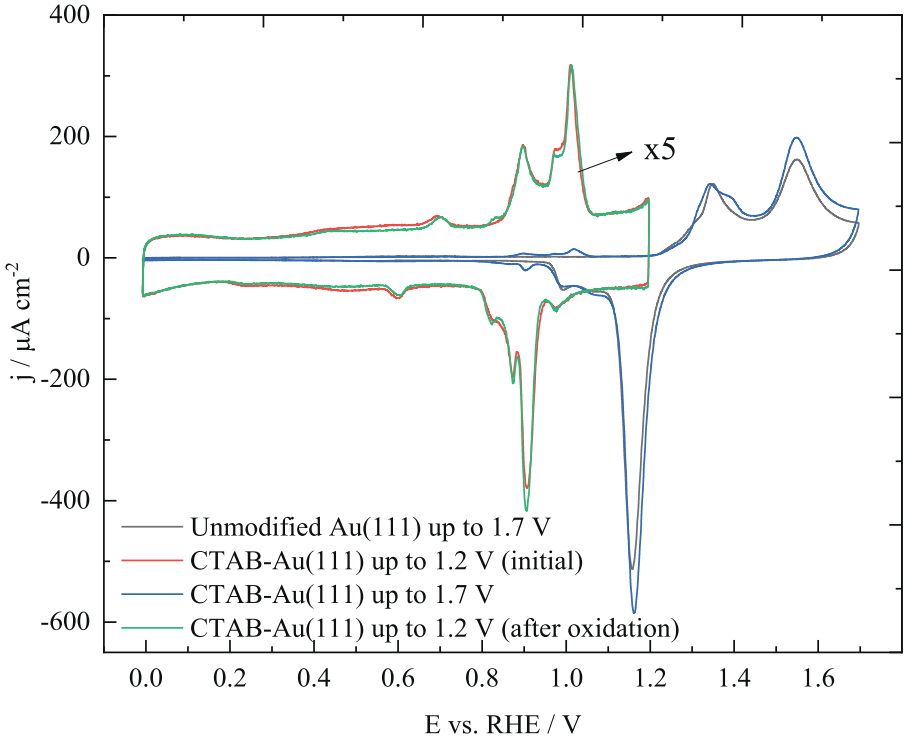

Figure 2. Voltammetric profiles of the unmodified and CTAB modified Au(111) electrode in 0.1 M $HClO_4$ up to 1.7 V and 1.2 V. The profiles for the CTAB-Au(111) up to 1.2 V and that recorded in the same potential region after the oxidation have been enlarged 5 times to better observe the peaks. Scan rate: 50 mV s^{-1}.

To get additional insight into the electric field across the interphase, the values of the thermal coefficient, ($\frac{\partial E}{\partial T}$), can be obtained. These values can be calculated from the transients according to the procedure described in detail in [24,25]. In summary, when the potential response to the temperature is fast, the transient ΔE vs t can be modeled using the following expression:

$$\Delta E = \frac{1}{2}\left(\frac{\partial E}{\partial T}\right)\Delta T_o\sqrt{\frac{t}{t_o}} \quad (1)$$

where ΔT_o is the initial temperature change after the pulse and t_o is the duration of the laser pulse (5 ns in this case). ΔT_o can be obtained from the laser intensity, the reflectivity of the surface, and the values of the thermal diffusivity and thermal conductivity of the metal and the aqueous solution according to the expression described in [24,25]. For the present conditions, this value of ΔT_o stands for 26.4 K. Then, the values of the thermal coefficient can be obtained from the slope of ΔE vs. $t^{1/2}$.

A brilliant Q-switched Nd:YAG laser (Quantel) was used for the litjm measurements. It delivers 5 ns laser pulses at a frequency of 532 nm. To regulate the temperature jump on the electrode surface, the energy of the laser was limited to 16 mJ cm^{-2} by combining the effect of an attenuator from Newport Corporation (Model M-935-10) and the Q-switched time. Laser pulses were synchronized with the transient measurements by the use of a Tektronix Model TDS 3054B oscilloscope and a potentiostat-galvanostat. In general, 250 potential transients at each desired potential were averaged by the oscilloscope The laser energy was measured by collecting the beam in a pyroelectric sensor head (Model LM-P10i). Additionally, the diameter of the laser (4 nm) was controlled to match the diameter of the electrode (ca. 2.5 mm) by a system of lenses.

3. Results and discussion

3.1. Behavior of CTAB/CTAOH on the Au(111) electrode in acidic solutions

Previous work has shown that CTA^+ forms adlayers on the Au(111) surface [21]. The adsorption of CTA^+ is carried out at open circuit from a solution containing 1 mM CTAB or CTAOH. After the adsorption, the electrode was transferred to the electrochemical cell, where the adlayer was characterized in 0.1 M $HClO_4$. The stable voltammetric profiles of the modified electrodes are shown in figures 1A and 2. As can be observed, the adlayer is stable in the whole potential window between hydrogen evolution and water oxidation. It should be noted that the initial profiles obtained after the immersion of the electrode in the case of the adlayer formed in CTAB solutions are different and evolve upon cycling. This evolution is due to the progressive desorption in the low potential range of the Br^- anions that were initially incorporated into the adlayer. Eventually, the stable profile is obtained.

Although the adlayer is stable in the whole potential window, its configuration changes with the electrode potential. Thus, the distance between the adlayer and the electrode surface is governed by the surface charge of the electrode. At potentials negative to the pzc, the CTA^+ adlayer is attracted to the surface through coulombic interactions, whereas when the surface charge becomes positive, the adlayer detaches from the surface, giving rise to the peaks at 0.8-0.9 V [21]. These peaks are due to the permeation of water and ions through the adlayer species and the subsequent change of the capacitance of the interphase (figure 1A). Above 1.2 V since the Au(111) electrode is in contact with a layer of electrolyte, the oxidation of the surface takes place in similar conditions to those obtained for the unmodified electrode. Thus, the voltammetric peaks corresponding to the oxidation/reduction process of the Au(111) surface for the CTA^+ modified electrodes are nearly identical to those obtained for the unmodified electrode.

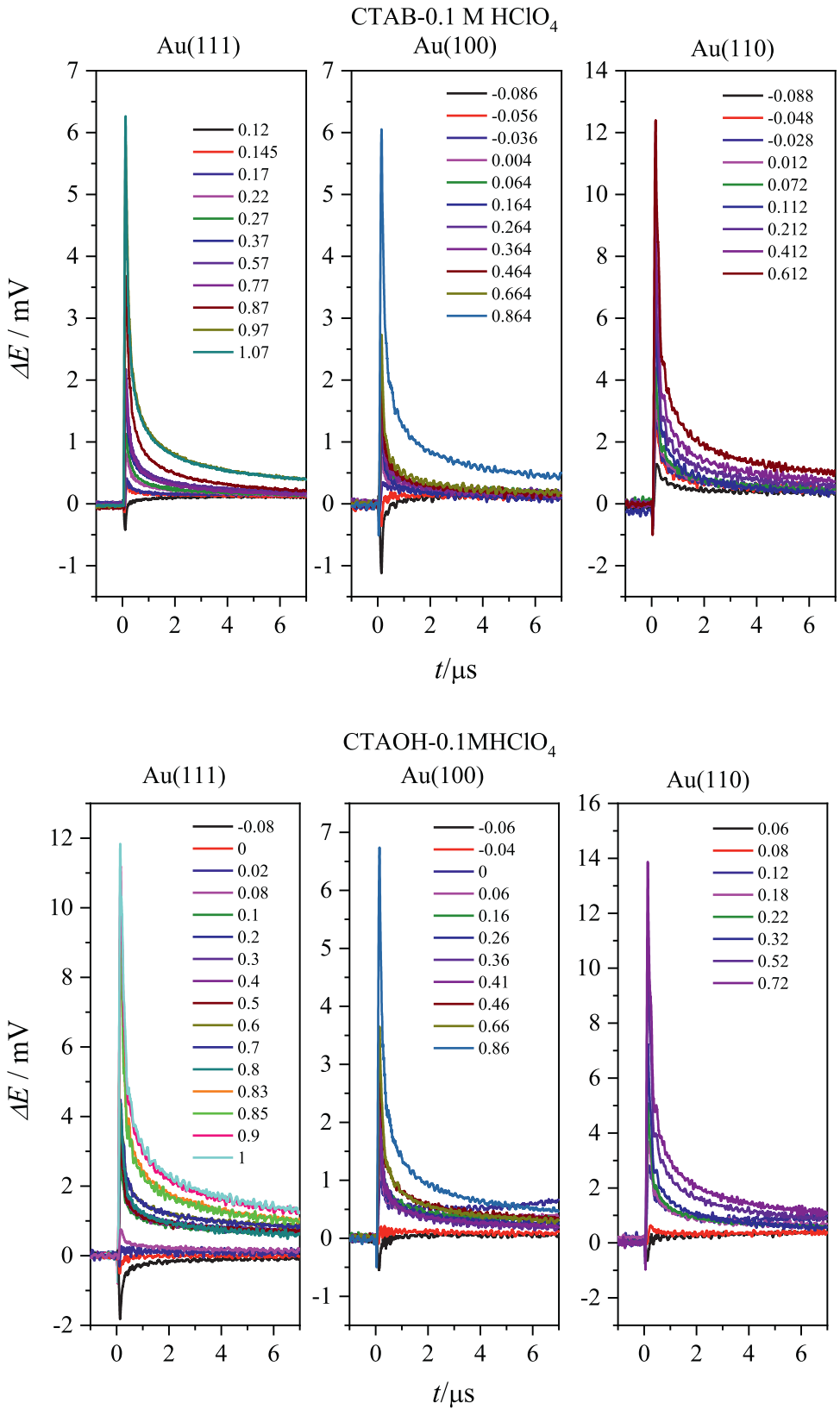

Figure 3. ΔE vs. time laser-induced transients recorded for the gold single crystal electrodes modified with CTAB or CTAOH layers. Laser beam energy: 2 mJ/pulse.

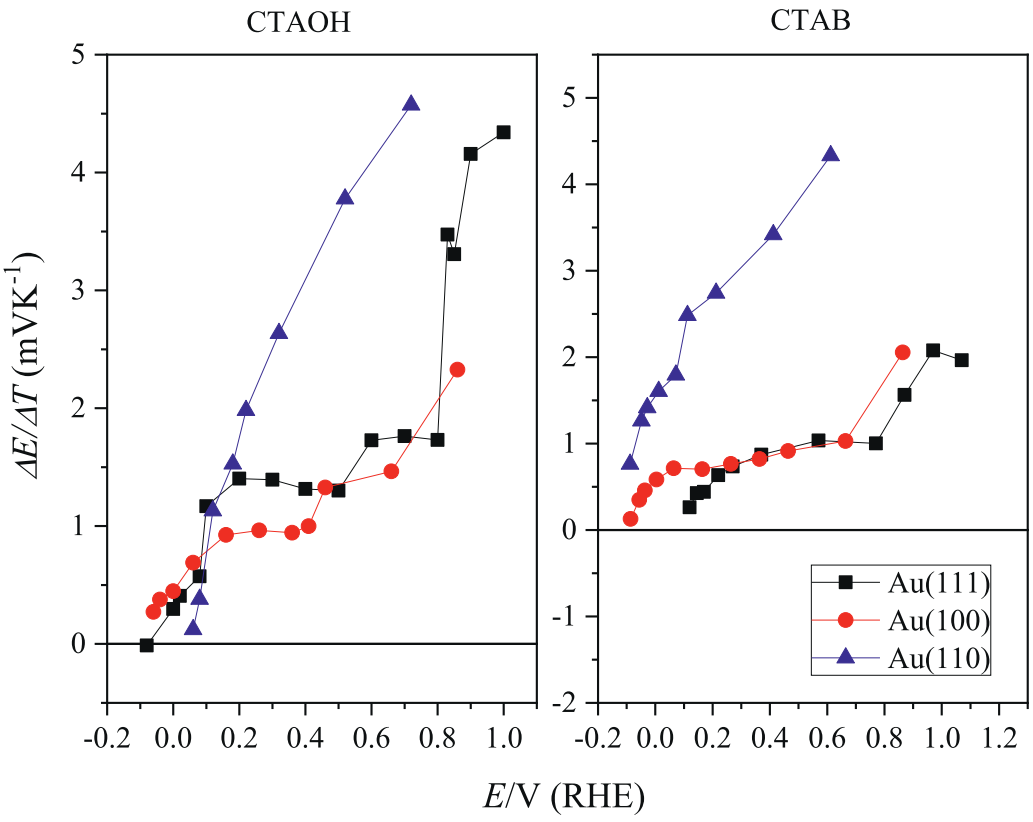

Figure 4. Thermal coefficients for the gold single crystal electrodes modified by CTAB and CTAOH layers obtained from the transients in figure 3.

Moreover, the surface oxidation/reduction process does not affect the stability of the adlayer, as can be deduced from the invariability of the voltammetric profiles in the region where $E<1.2$ V before and after the oxidation. It should be noted that the voltammetric differences between the adlayer formed in CTAB and CTAOH solutions are small, indicating that the adlayers have similar properties, despite being formed from different solutions. Also, the concentration of the CTAB/CTAOH solution used for the formation of the adlayer and the immersion time has also no effect in the range between 0.1-10 mM, (Figures S1-S2), since the voltammograms are almost independent of the immersion time and concentration, implying that the adlayer has reached the maximum coverage under the present conditions. Additionally, since the critical micellar concentrations are ca. 1 mM and 0.86 mM for CTAB and CTAOH, respectively, the presence of micelles in the solution does not affect the formation of the adlayer. This result indicates that hemimicelles are not formed during adsorption. Although the concentration of CTAB/CTAOH in the solution where the adlayer is formed does not affect it significantly, for all the figures displayed in this manuscript the CTAB/CTAOH concentration was 1 mM and the electrode was immersed for 15 s in the corresponding solution.

Additional information on the structure of the adlayer can be obtained from the charge analysis. The charge is obtained from the integration of the voltammetric profiles, using an integration constant. For the unmodified Au(111) electrode, the integration constant is easily obtained because the charge should be zero at the potential of zero charge. Due to the reconstruction phenomena of the Au single-crystal surfaces [26-28], two pzc's have been reported, one for the unreconstructed (1×1) surface (pzc_u) and one ($22\times\sqrt{3}$) for the reconstructed surface (pzc_r) [29-31]. The stability domains of each surface structure are determined by the surface charges and thus, the ($22\times\sqrt{3}$) is favored when the surface charge is negative whereas the (1×1) structure is stable at positive potentials [32,33]. The transition between both structures is determined mainly by the kinetic of the processes, being the lifting of the reconstruction a fast process and the reconstruction a slow one [32]. This difference in the kinetics of both processes gives rise to unsymmetrical (with respect to the x-axis) voltammetric profiles. In this sense, it can be considered that the profiles in the negative scan direction correspond mainly to the unreconstructed surface. For this reason, the negative scan direction has been integrated for the charge analysis. For the CTAB/CTAOH Au(111) modified surface, it has been assumed that the charge at 1.2 V, i.e., the potential at which the adlayer is detached from the surface, is the same as that obtained for the unmodified surface. It should be remembered that the voltammetric profiles above 1.2 V for the CTA^+ modified electrodes and the unmodified Au(111) surface are almost identical, which supports this charge value assignment.

Charge curves for the Au(111) electrodes are shown in figure 1B. For the modified electrodes, the charge curve crosses the zero value at ca. 0.70 V, that is, just at the onset of the peaks that mark the detachment of the adlayer from the Au(111) surface. This would suggest that the pzc for these modified electrodes has been displaced to more positive potentials with respect to the unmodified electrode. The displacement of the pzc to more positive potentials is the expected consequence of the specific adsorption of cations on the electrode surface. However, due to the complex nature of the adlayer, in which anions should be involved in the stabilization of the adlayer, additional information from the interphase is required in order to determine the surface charge of the electrode and the interfacial field. It should be noted that the charge analysis carried out here cannot distinguish between the free charge of the electrode, which generates the electric field in the interphase, and that due to the adsorption processes of the different surface species. This difference is especially important for metals, such as platinum, with a large adsorption capacity. For this latter type of metals, two pzc can be defined: the potential of zero free charge (pzfc) and the potential of zero total charge (pztc) [34].

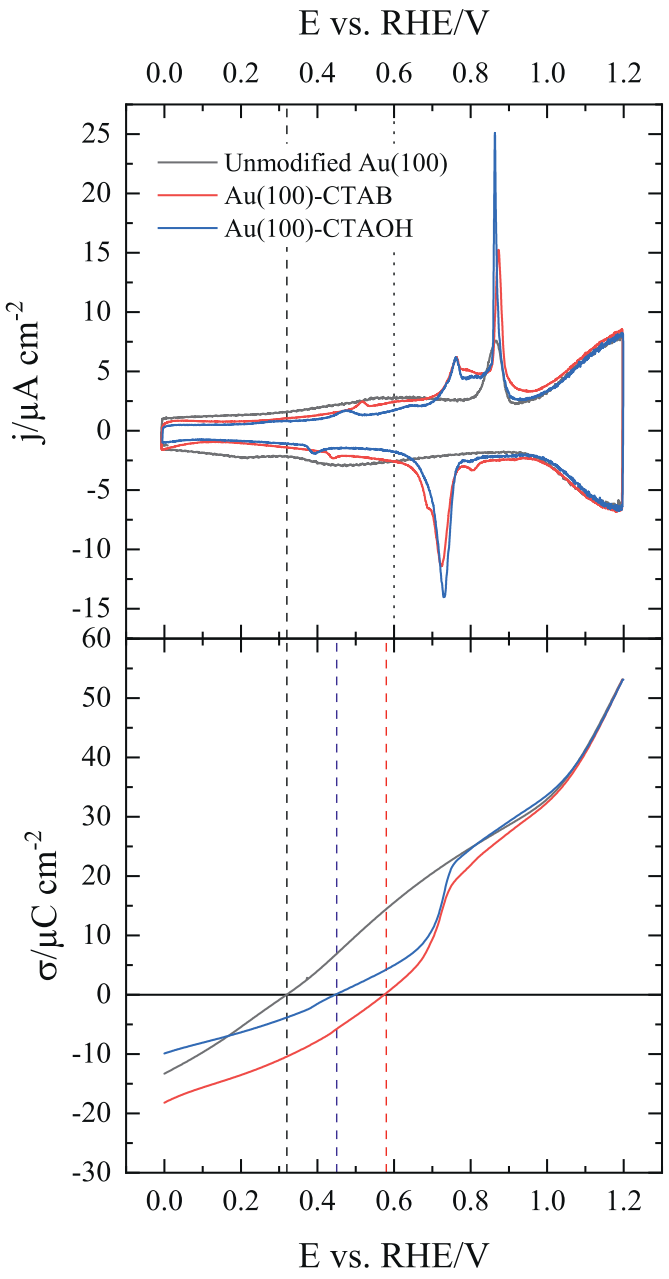

Figure 5. A) Stable voltammetric profile for the unmodified Au(100) electrode and the CTAB and CTAOH modified Au(100) electrodes in 0.1 M $HClO_4$. The vertical lines mark the position of the pzc_u (dashed line) and pzc_r (dotted line) of the unmodified Au(100) surface. B) Charge curves obtained from the voltammetric profiles. The vertical lines reflect the point at which the curves cross the zero charge value.

The pzfc is the potential at which the surface charge is zero and, thus, the field across the interphase is also zero. It is the equivalent to the pzc of non-adsorbing metals, such as gold. On the other hand, the pztc is the potential at which the charge of the interphase plus the charge exchanged in the adsorption processes is null. In these cases, the pztc is the value that can be directly measured, whereas the determination of the pzfc requires non-thermodynamic assumptions.

One of the methods that can be used to estimate the pzfc is litjm described above because the potential transients recorded in coulostatic conditions reflect the changes in the orientation of water molecules in the interphase upon the heating process due to the laser pulse. Thus, the potential at which the transient is zero corresponds to a situation in which water molecules are not preferentially oriented and the entropy of formation of the interphase is maximum, that is, the potential of maximum entropy (pme). The pme is very close to the pzfc because the electric field is the major force in the orientation of the water molecules in the interphase [24,25]. For gold, which is considered a non-adsorbing metal, the pme and pzc differ in less than 50 mV.

Transients using the litjm for the CTA^+ modified electrodes were recorded, as shown in figure 3. As can be seen, the pme for the Au(111) modified electrodes are ca. 0.10 and 0.02 V for the CTAB and CTAOH modified electrodes, respectively. The large difference between these pme values and those for which the charge is zero measured from figure 1B clearly indicates that the adlayer structure is complex, containing not only the CTA^+ cations but also additional species, probably anions, and water molecules. At the pme, the electrochemical behavior and the in-situ FTIR spectra shows that CTA^+ adlayer is attached to the surface with the amino group close to the surface and the long alkyl chain (tails) pointing out towards the solution [21]. Due to the hydrophobic nature of the tails, water molecules are most likely excluded from the molecular adsorbed layer, and, thus, the litjm experiments should reflect mainly the change in the orientation of water molecules on top of the adlayer. When the CTA^+ adlayer is attached to the surface, the electric field on the water molecules in the interphase is the result of the net charge resulting from three contributions: the surface charge, the adsorbed CTA^+ cations, and also the possible anions involved in the stabilization of the adlayer. The water on top of the adlayer is mainly responding to the overall charge resulting from these three contributions. On the other hand, the pzc value obtained from the integration of the voltammogram would contain only the surface charge, assuming that, in the attachment of the CTA^+ adlayer to the surface, no faradaic process is involved, i.e., the charge of the CTA^+ adlayer is considered part of the solution side of the interphase. Thus, at 0.7 V and to compensate the overall positive charge of the CTA^+ adlayer, the surface charge becomes negative. However, the interfacial water is still experiencing a positive charge because the sum of the surface charge plus the charge of the CTA^+ cations and the anions in the adlayer is still positive. The opposite effect was described for the adsorption of anions on Au(111) or Pt(111) that turns the laser-induced potential transients negative at potentials above the pzc where they should be positive [24,25]. The coadsorption of anions has already been proposed for other quaternary ammonium salts on Au(111) electrodes, in which the formation of an ion-pair in the adlayer has been suggested [35]. In fact, this ion-pair formation can explain the stability of the adlayer on the surface in perchloric acid solutions, since cetyltrimethylammonium perchlorate is an insoluble salt.

Additional information can be obtained from the thermal coefficients obtained from the transients (fig. 4). As can be seen, the thermal coefficients for the Au(111) electrode in the region between 0.6-0.8 V in which the peaks appear to show a large variation, reflecting the interfacial changes due to the attachment/detachment of the CTA^+ adlayer.

3.2. Behavior of CTAB/CTAOH on the Au(100) electrode in acidic solutions

The same experiments for the Au(111) were repeated for the Au(100) electrodes. In figure 5, the voltammograms under the different conditions are shown. It should be also noted that the Au(100) surface is also affected by reconstruction phenomena [36-39]. After the annealing and at low potentials, the top-most layer of the surface adopts a hexagonal arrangement, very similar to that of the (111) surface, whereas at positive potentials with respect to the pzc, the nominal (1×1) surface structure is obtained. In the positive scan direction, the lifting of the reconstruction is signaled by the peak appearing at 0.80 V.

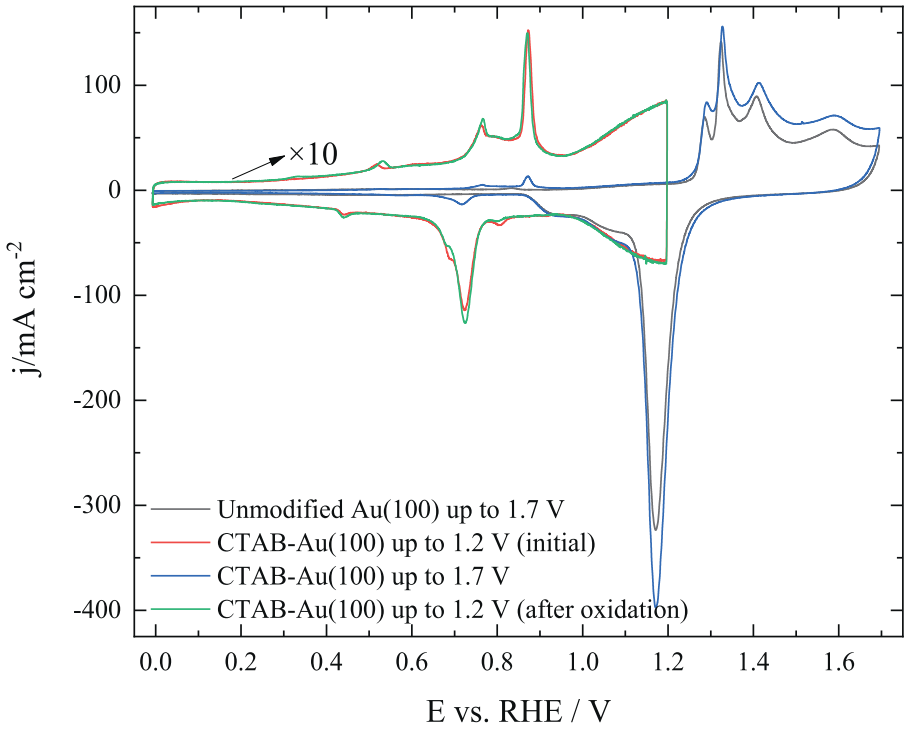

Figure 6. Voltammetric profiles of the unmodified and CTAB modified Au(100) electrode in 0.1 M $HClO_4$ up to 1.7 V and 1.2 V. The profiles for the CTAB-Au(100) up to 1.2 V and that recorded in the same potential region after the oxidation have been enlarged 10 times to better observe the peaks. Scan rate: 50 mV s^{-1}.

As can be seen in figure 5A, the modification of the Au(100) electrode with the CTAB/CTAOH leads to the appearance of new peaks in the region between 0.6-0.9 V. Moreover, at potentials more positive than 0.9 V, the voltammograms of the unmodified and CTA^+ modified surfaces are almost identical. In this case, the peaks in the region of 0.6-0.9 V have a different morphology than those observed for the Au(111) surface. However, the qualitative behavior is the same as that observed for the Au(111) electrode, although, the process giving rise to those peaks appears to be more irreversible, peak potentials and their multiplicity are also different. For the Au(100), a peak at 0.79 followed by a very sharp peak at ca. 0.88 V is seen in the positive scan direction. This latter peak coincides with the peak associated with the lifting of the reconstruction in the unmodified surface. Conversely, a single peak is observed in the negative scan direction at 0.73 V.

When the scan is extended up to the region in which the surface is oxidized, the voltammograms in figure 6 show the same behavior as that reported for the Au(111) electrode, that is, the voltammetric profile in the region for E>1.2 V is nearly the same as that observed for the unmodified electrode. This fact suggests that the mechanism explaining the adlayer behavior on the Au(111) electrode is also applicable to the Au(100) electrode. Thus, at potentials negative to the pzc, the CTA^+ adlayer is attached to the Au(100) surface. As the potential increases and the surface charge becomes positive, the adlayer detaches. This mechanism can also explain the difference in the irreversibility of the peaks for the Au(111) and Au(100) electrodes, because, at positive potentials, the surface is unreconstructed whereas at negative potentials the reconstructed surfaces are slowly formed. For the Au(100), the pzc of the reconstructed surface is ca. 0.24 V more positive than that of the unreconstructed surface, whereas for the Au(111), the difference between the pzc of the reconstructed and unreconstructed surfaces is ca. 0.1 V. The larger irreversibility of the peaks in the Au(100) electrode can be related to the larger difference in energetics between the unreconstructed and reconstructed surfaces on the Au(100) electrode, as the position of the pzc's shows.

Charge measurements were also carried out for this electrode, using the same protocol applied for the Au(111) electrode. In general, the results show a similar trend to that observed for the Au(111), that is, the potential at which the charge becomes zero shifts to more positive potential values, as expected for a layer formed by cations. In this case, the potential at which the charge is zero for the adlayer formed in the CTAOH solutions is at significantly lower potential values than that for the CTAB adlayer. The difference may arise from small modifications in the adlayer structure due to the different environments in which they were formed. Thus, the adlayer formed in the CTAOH containing solution has shaper peaks and slightly smaller currents at low potentials, where pure capacitive processes are observed. This behavior is normally associated with a more compact adlayer or a less defective one.

On the other hand, the litjm experiments, which serve to determine the charge of the electrode+adlayer, provide a value for the pme which is significantly more negative than the pzc of the unmodified surface (figure 3). In fact, for the modified electrodes, the pme is very close to 0, clearly showing that the negative charge present in the unmodified Au(100) electrode is compensated by the positive charge of the CTA^+ adlayer so that the electric field that the water molecules above the adlayer experienced is zero. Also, the major changes in the thermal coefficients obtained from the transients are observed in the region where the peaks are located, a clear indication that major changes in the structure of the interphase are taking place during those peaks.

3.3. Behavior of CTAB/CTAOH on the Au(110) electrode in acidic solutions

The (110) surface of fcc metal is complex because it can also be considered as a stepped surface having 2 atom-wide (111) terraces separated by monoatomic (111) steps. This type of surface gives rise to an open structure in which the second layer of atoms is "accessible" from the surface. Moreover, the Au(110) surface ex-

periences a (1×2) reconstruction, also known as missing row, in which every other row is eliminated, giving rise to a stepped surface with 3 atom-wide (111) terraces separated by diatomic (111) steps [40,41]. As happens with the other two basal planes of gold, the (1×2) reconstruction is stable only at potentials negative to the pzc. However, in this case, the voltammogram in perchloric acid solution is almost reversible with respect to the x-axis (figure 7) and no specific signals can be associated with the lifting of the reconstruction. It should be noted that the energetics of the reconstructed and unreconstructed surfaces are very similar because the value of the pzc for both structures is almost the same [42]. Thus, the expected changes in the interaction of the surface with the species in the interphase should be almost negligible.

The modifications observed in the voltammograms when the electrode is immersed in the CTAB/CTAOH solutions are much less defined than those observed in the previous electrodes (figure 7). In fact, only broad signals can be observed in the voltammogram, which are different from those observed for the unmodified surface. In any case, the double layer current at low potentials is smaller than that recorded for the unmodified surface, which reveals the presence of an adsorbed layer. The absence of pronounced peaks in the voltammograms of the modified Au(110) electrodes results in charge curves that are very similar to those obtained for the unmodified surface. As expected, the potential for which the charge for the modified electrode is zero is slightly more positive than that measured for the unmodified electrode. These results indicate that the modification of the electrode properties by the adsorption of the CTA^+ species is less important than in the previous cases, probably reflecting the more complex nature of the surface. On the other hand, the presence of the adlayer is evident in the litjm measurements. The pme measured for these adlayers with the litjm are displaced to negative values, in agreement with the results for the other surfaces, indicating that the qualitative behavior of the adlayer is the same, independently of the symmetry of the electrode surface. However, the changes in the thermal coefficients are gradual without any steep increase as those observed for the other two electrodes in the same potential region where the peaks appear. This fact suggests that the changes in the distance of the adlayer are also gradual with the electrode potential, in agreement with the absence of sharp and well-marked peaks in the voltammogram.

When the upper electrode potential is set in the oxide region, the voltammogram of the modified Au(110) electrode is almost identical to that obtained for the unmodified surface (figure 8), as happens with the other basal planes. However, the voltammetric profile after the oxidation shows some changes, with the loss of some of the previous characteristics, probably due to the partial desorption/oxidation of the adlayer. This fact could be related to the open nature of the topmost layer of the Au(110), in which the interaction of the adsorbed molecules with the second layer of Au is possible. Thus, the distances between the different atoms exposed on the surface and the adlayer are not uniform, and some interaction between the adsorbed OH and the CTA^+ layer is possible, giving rise to partial desorption upon oxidation.

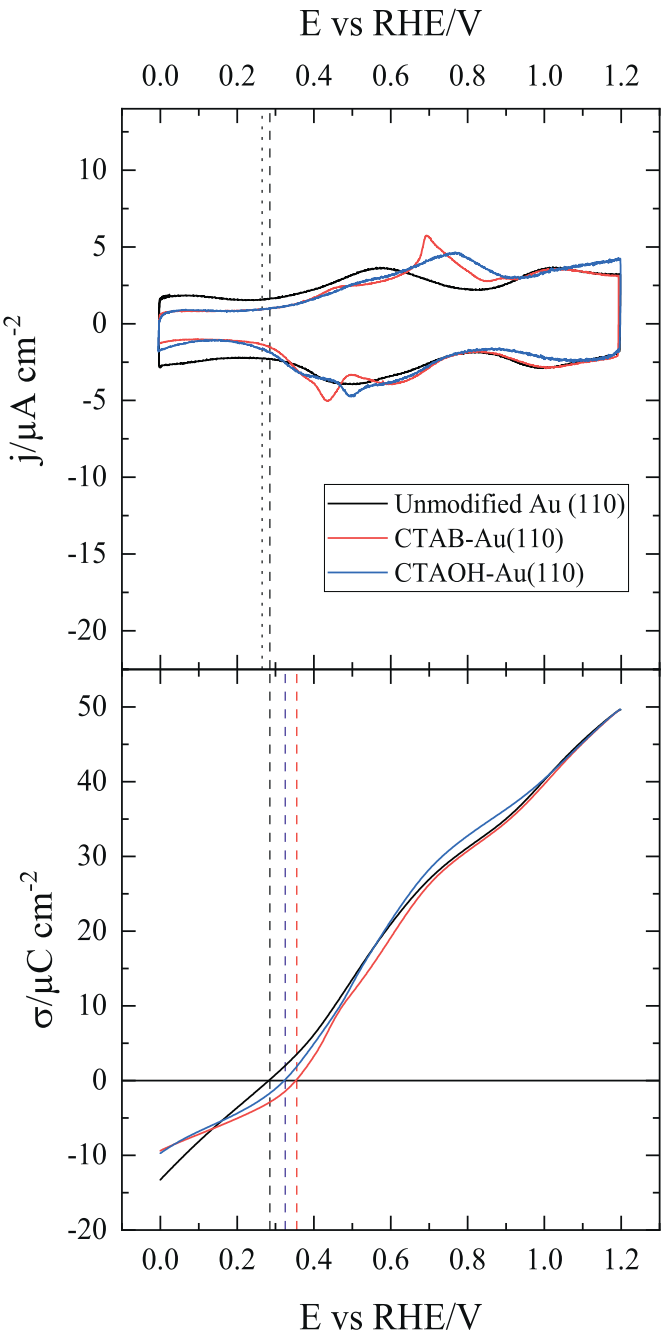

Figure 7. A) Stable voltammetric profile for the unmodified Au(110) electrode and the CTAB and CTAOH modified Au(110) electrodes in 0.1 M $HClO_4$. The vertical lines mark the position of the pzc_u (dashed line) and pzc_r (dotted line) of the unmodified Au(110) surface. B) Charge curves obtained from the voltammetric profiles. The vertical lines reflect the point at which the curves cross the zero charge value.

3.4. The behavior of the CTAB/CTAOH layers in NaOH solutions

Previous results have shown that the potentials for the peaks related to the permeation of water through the adlayer are associated with an increase of the distance between the adlayer and the electrode surface are independent of the pH in the SHE scale in acidic solutions [21]. These results demonstrated that this process is governed by the electrode charge. Thus, at positive charges, the CTA^+ adlayer is repelled, and at negative charges, the adlayer is attracted towards the surface. In alkaline media, the electrode charge at E<1.2 V (RHE) is always negative, and it would be expected that the adlayers were stable in this potential range and remain in contact with the electrode surface preventing any electrochemical adsorption process from the anions of the supporting electrolyte. However, the observed results are different. Figure 9 shows the voltammograms for the CTAB/CTAOH modified electrodes. As can be seen, the modifications of the profiles after the formation of the adlayer are small. In the case of the Au(111) and Au(100) electrodes, the signals due to the lifting of the reconstruction, triggered by the initial adsorption of OH, are somehow smaller than those recorded in the absence of the adlayer. The appearance of these

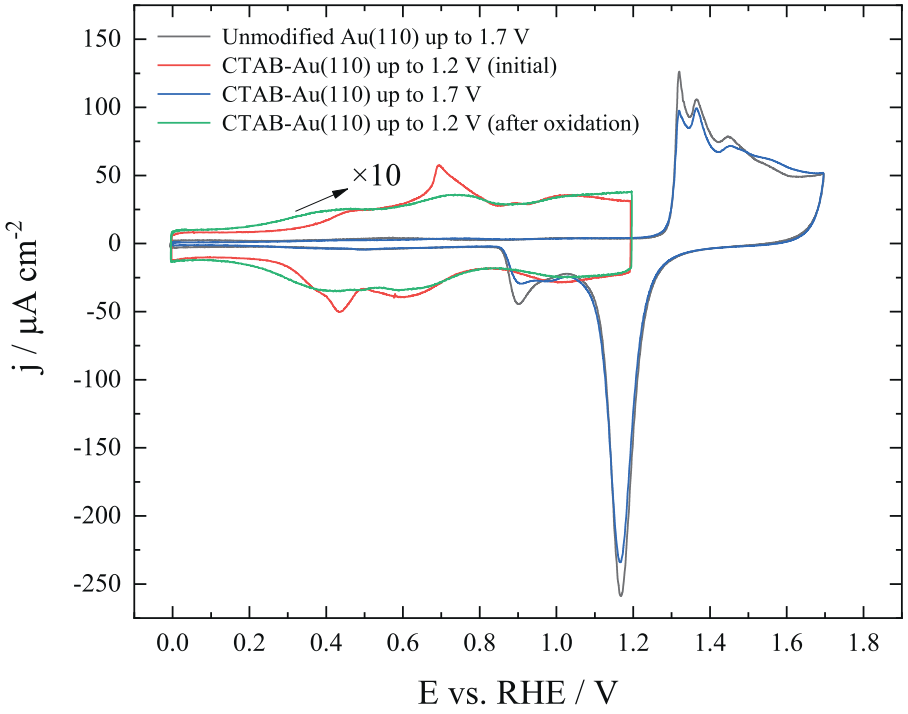

Figure 8. Stable voltammetric profiles of the unmodified and CTAB modified Au(110) electrode in 0.1 M $HClO_4$ up to 1.7 V and 1.2 V. The profiles for the CTAB-Au(110) up to 1.2 V and that recorded in the same potential region after the oxidation have been enlarged 10 times to better observe the peaks. Scan rate: 50 mV s^{-1}.

initial signals related to the adsorption of OH on both electrodes clearly indicates that the coverage of the CTA^+ is small, because, otherwise, the adsorption of the OH would have been inhibited by the presence of an adsorbed adlayer in close contact with the electrode surface. Moreover, the profile in the surface oxidation region (figures S3) is almost identical to those obtained in the absence of the adsorbed adlayer. These results point out that the adlayer has been partially desorbed after its transfer to the alkaline solutions. In order to get additional insight into this process, the effect of pH and ionic strength of the solution was examined. As can be seen in figure S4, coverages of the adlayer increase with the diminution of the pH and the increase of the ionic strength, clearly indicating that the adlayer is not stable in very alkaline solutions.

The major difference between perchloric and NaOH solutions regarding CTAB and CTAOH is that these species are insoluble in perchloric acid but soluble in NaOH solutions. Thus, it can be proposed that the reason for the lower coverages is the partial desorption of the adlayer due to dissolution. In order to corroborate this, 1 mM CTAB and CTAOH were dissolved in 0.01 M NaOH solutions and the voltammograms in these solutions were recorded. As can be seen in figure 10, the profiles in this solution are completely different from those recorded previously. In this case, the peaks related to the lifting of the reconstruction are completely suppressed. Moreover, when CTAB is present in the solution, additional sharp peaks are observed, which are absent in the CTAOH solution. In this latter case, only small peaks are observed in the voltammetric profile at low potentials. Thus, these peaks observed in the presence of CTAB in solution have to be related to the presence of Br^-, indicating that the anion has also a role in the formation and stabilization of the adlayer. Probably, those peaks are due to the adsorption/desorption of Br^- anions in the adlayer. For the Au(100) electrode, the qualitative behavior (figure S5) is the same, that is, a larger coverage is obtained and significant differences in the behavior of the CTAB and CTAOH solutions are observed. These effects have been also observed for the adsorption of quaternary ammonium salts with shorter alkyl chains. The presence of a shorter alkyl chain increases the solubility of the adlayer, and a reversible

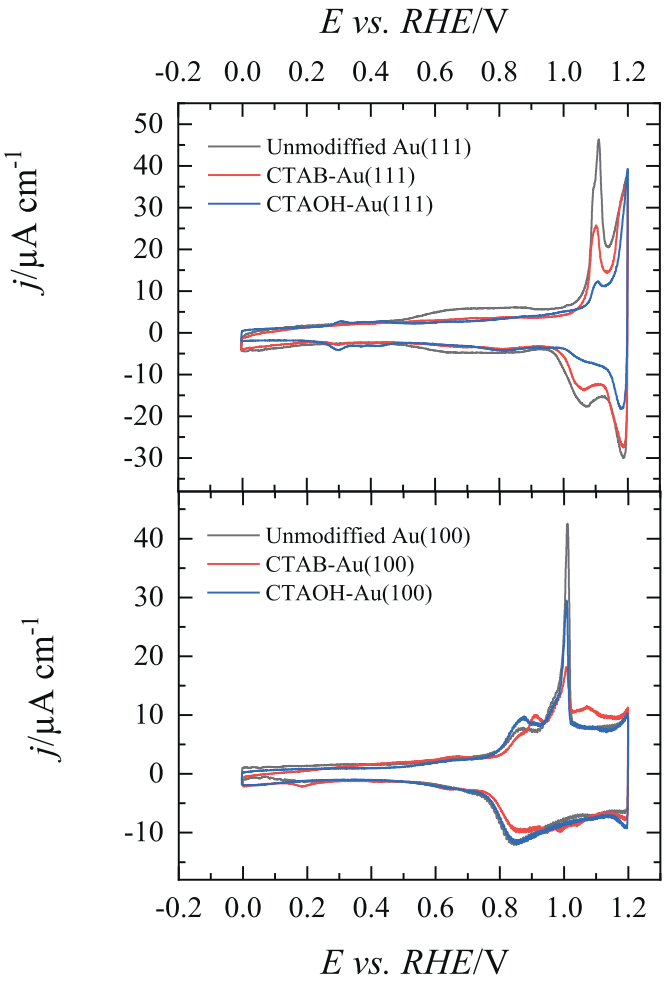

Figure 9. Stable voltammetric profiles for the unmodified Au(111) and Au(100) electrodes and the CTAB and CTAOH modified electrodes in 0.1 M NaOH.

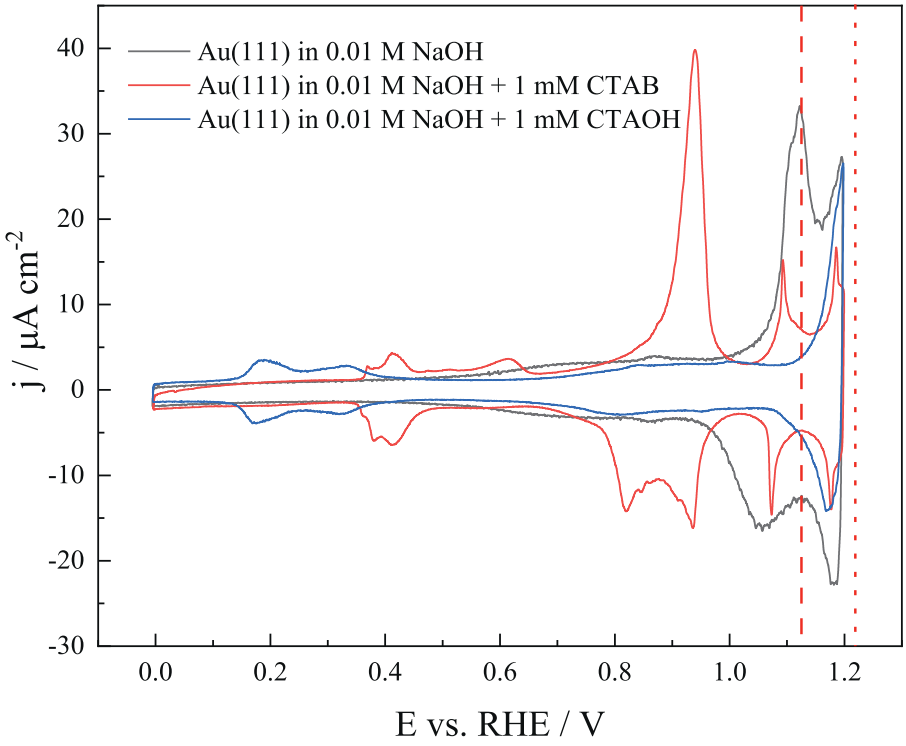

Figure 10. Stable voltammetric profile for the Au(111) electrode in 0.01 M NaOH in the absence and presence of 1 mM CTAB or 1 mM CTAOH in solution. Scan rate 50 mV s^{-1}.

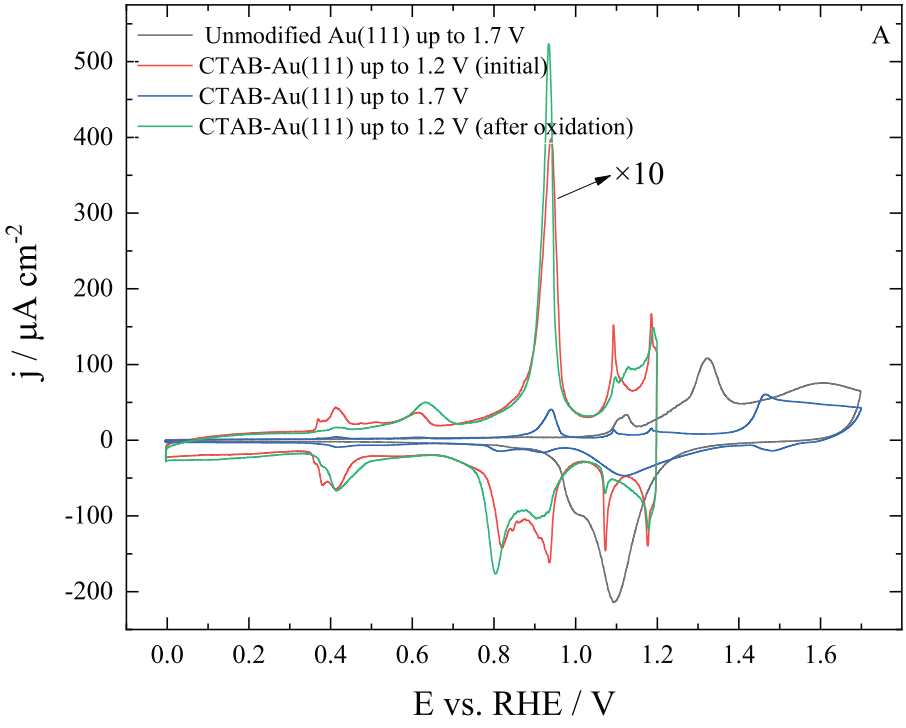

Figure 11. Stable voltammetric profiles for the Au(111) electrode in 0.1 M NaOH in the absence and presence of 1 mM CTAB up to 1.7 V and 1.2 V. The intial profile for the CTAB-Au(111) up to 1.2 V and that recorded in the same potential region after the oxidation have been enlarged 10 times to better observe the peaks. Scan rate: 50 mV s^{-1}.

adsorption behavior is observed even in neutral conditions. Under these circumstances, the presence of bromide modifies the adsorption behavior due to the coadsorption of the bromide anion and the quaternary ammonium cation [43,44]. Also, for these salts, the peaks at low potentials (as those observed in figure 10) are related to the desorption of the adlayer [45]. All these results indicate that the adsorption behavior of the quaternary ammonium salts is the result of a delicate balance between the mutual interactions of the quaternary ammonium cation, the counter-anion, the electrode surface, and the water molecules.

Additional information can be obtained when the electrode potential is scanned in the oxide formation region. As can be seen in

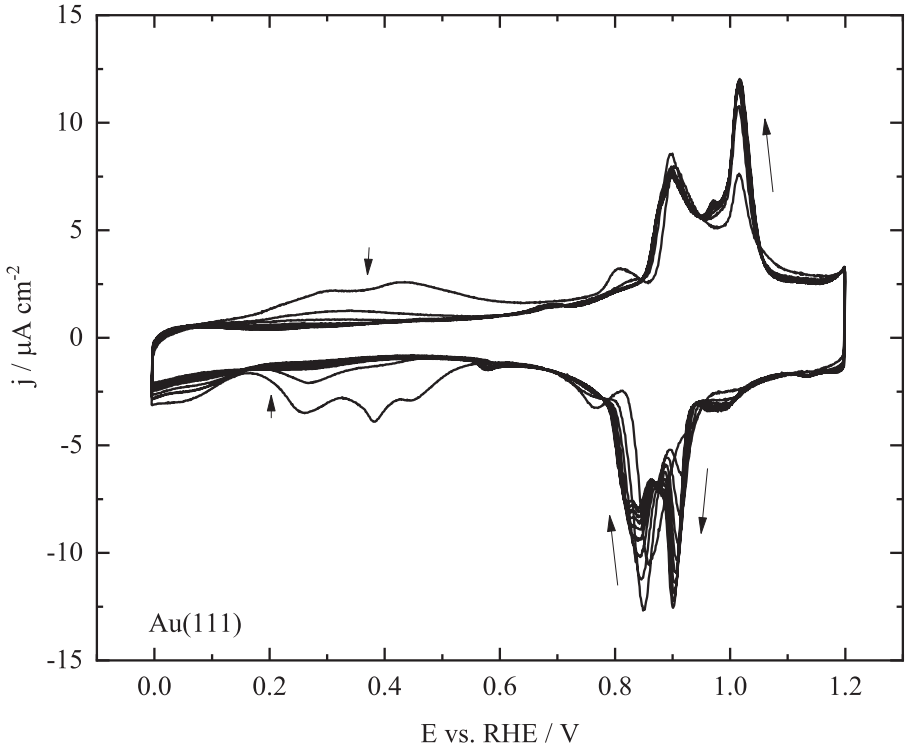

Figure 12. Evolution of the profile of the CTAB modified Au(111) electrode upon cycling in 0.1 M $HClO_4$ after the transfer from a solution containing 0.01 M NaOH and 1 mM CTAB. The arrows show the evolution of the profile. Scan rate: 50 mV s^{-1}.

figure 11 for the Au(111) and in figure S6 for the Au(100), the formation of the oxide is inhibited and the profile differs significantly from that obtained in absence of CTAB/CTAOH. This is the expected behavior of the adlayers, because the attractive interaction due to the negative charge on the electrode surface and the positive polar heads of the CTA^+ cations hinders the adsorption of OH and eventually the surface oxidation process. Thus, the lower coverage of the CTA^+ layers obtained in figure 9 is due to the dissolution of the adlayer. Moreover, the profile after the oxidation changes, a clear indication that the oxidation of the surface also leads to the partial oxidation of the adlayer and a modification in its structure. Since the adlayer is in contact with the surface when the adsorption of OH takes place, the interaction of adsorbed OH and CTA^+ favors its oxidation process.

Further proofs of the similar nature of the formed adlayers in alkaline solution are obtained when the electrode is transferred to a 0.1 M $HClO_4$ solution (figure 12). The electrode is emersed at 1.2 V (RHE) from the 0.01 M NaOH solution and immersed at the same potential (RHE scale) in the 0.1 M $HClO_4$ solution. As can be seen, the voltammetric profile evolves to the stable profile obtained in this solution, shown in figure 1. The initial currents observed at low potentials are corresponding to the gradual desorption of the Br^- anions, in a very similar evolution of the profile as that obtained when the adlayer is formed in neutral solutions (see figure 1A in reference [21]). Similar behavior is observed for the Au(100) electrode (figure S7).

4. Conclusions

The results presented here show the complex behavior of the CTA^+ adlayers adsorbed on the Au electrode surface. At potentials below the pzc of the clean Au surface, the adlayer is in contact with the surface because the negative charge of the electrode attracts the positive polar heads of the CTA^+ cations. As the surface charge becomes positive, the adlayer detaches from the surface and water molecules permeate through it, so that the behavior of the electrode covered by the adlayer is almost identical to that obtained in its absence, as the voltammetric profiles for the oxidation of the surface show. However, if the electrode charge becomes negative again, the adlayer re-attaches to the electrode surface.

Charge measurements and litjm show that the composition of the adlayer contains not only the CTA^+ cations but also anions. The charge measurements show that the potential at which the total charge zero shifts to more positive potentials, in agreement with the expected results for an adlayer formed by cations. However, the analysis of the electric field above the adlayer, which can be assessed by the litjm, shows that the water molecules on top of the adlayer experience a positive charge at those potentials. Thus, the CTA^+ adlayer must also contain anions, which neutralize part of the positive charge of the adlayer, in such a way that the field experienced by the water molecules on top of the adlayer is still negative. The anions probably also serve to stabilize the adlayer. This behavior of the adlayer is observed in the whole pH window. However, the higher solubility of CTAB/CTAOH in alkaline solutions leads to the desorption of the adlayer when these species are not present in the solution. When CTAB and CTAOH are dissolved in the electrolytic solution, the behavior shows the formation of an adsorbed layer, which is strongly bonded to the surface due to the negative charge of the surface. Moreover, the differences between the behavior of CTAB and CTAOH reveal that the anion is involved in the adlayer. In fact, when the adlayer formed in the alkaline solution containing CTAB is transferred to a perchloric acid solution, the voltammograms show the gradual and progressive desorption of the bromide anions.

Declaration of Competing Interest

None.

Acknowledgments

Financial support from Ministerio de Ciencia e Innovación (Project PID2019-105653GB-I00) and Generalitat Valenciana (Project PROMETEO/2020/063) is acknowledged.

Authors contribution

All authors have contributed equally to this manuscript.

Declaration of Competing Interests

The authors declare that they have no known competing financial interests or personal relationships that could have appeared to influence the work reported in this paper.

Supplementary materials

Supplementary material associated with this article can be found, in the online version, at doi:10.1016/j.electacta.2021.138947.

References

[1] H. Leidheiser, Corrosion Control by Organic Coatings, National Association of Corrosion Engineers Houston, TX, USA, 1981.
[2] S. Casalini, C.A. Bortolotti, F. Leonardi, F. Biscarini, Self-assembled monolayers in organic electronics, Chem. Soc. Rev. 46 (2017) 40–71.
[3] J.J. Gooding, F. Mearns, W. Yang, J. Liu, Self-assembled monolayers into the 21st century: recent advances and applications, Electroanal 15 (2003) 81–96.
[4] J. Lipkowski, Biomimetics: a new research opportunity for surface electrochemistry, J. Solid State Electrochem. 24 (2020) 2121–2123.
[5] H. Heinz, C. Pramanik, O. Heinz, Y. Ding, R.K. Mishra, D. Marchon, R.J. Flatt, I. Estrela-Lopis, J. Llop, S. Moya, R.F. Ziolo, Nanoparticle decoration with surfactants: molecular interactions, assembly, and applications, Surf. Sci. Rep. 72 (2017) 1–58.
[6] A. Gole, C.J. Murphy, Seed-mediated synthesis of gold nanorods: role of the size and nature of the seed, Chem. Mater. 16 (2004) 3633–3640.
[7] C.J. Murphy, T.K. Sau, A.M. Gole, C.J. Orendorff, J. Gao, L. Gou, S.E. Hunyadi, T. Li, Anisotropic metal nanoparticles: synthesis, assembly, and optical applications, J. Phys. Chem. B 109 (2005) 13857–13870.
[8] B. Nikoobakht, M.A. El-Sayed, Preparation and growth mechanism of gold Nanorods (NRs) using seed-mediated growth method, Chem. Mater. 15 (2003) 1957–1962.
[9] J. Perez-Juste, I. Pastoriza-Santos, L.M. Liz-Marzan, P. Mulvaney, Gold nanorods: synthesis, characterization and applications, Coor, Chem. Rev. 249 (2005) 1870–1901.
[10] K. Park, L.F. Drummy, R.C. Wadans, H. Koerner, D. Nepal, L. Fabris, R.A. Vaia, Growth mechanism of gold Nanorods, Chem. Mater. 25 (2013) 555–563.
[11] S. Si, C. Leduc, M. Delville, B. Lounis, Short gold nanorod growth revisited: the critical role of the bromide counterion, ChemPhysChem 13 (2012) 193–202.
[12] X. Ye, L. Jin, H. Caglayan, J. Chen, G. Xing, C. Zheng, V. Doan-Nguyen, Y. Kang, N. Engheta, C.R. Kagan, C.B. Murray, Improved size-tunable synthesis of monodisperse gold nanorods through the use of aromatic additives, ACS Nano 6 (2012) 2804–2817.
[13] D.K. Smith, N.R. Miller, B.A. Korgel, Iodide in CTAB prevents gold nanorod formation, Langmuir 25 (2009) 9518–9524.
[14] J.E. Millstone, W. Wei, M.R. Jones, H. Yoo, C.A. Mirkin, Iodide ions control seed-mediated growth of anisotropic gold nanoparticles, Nano Lett 8 (2008) 2526–2529.
[15] N. Garg, C. Scholl, A. Mohanty, R. Jin, The role of bromide ions in seeding growth of Au Nanorods, Langmuir 26 (2010) 10271–10276.
[16] L. Wang, X. Jiang, J. Ji, R. Bai, Y. Zhao, X. Wu, C. Chen, Surface chemistry of gold nanorods: origin of cell membrane damage and cytotoxicity, Nanoscale 5 (2013) 8384–8391.
[17] R. del Caño, J.M. Gisbert-Gonzalez, J. Gonzalez-Rodriguez, G. S.-O., R. Madueño, M. Blazquez, T. Pineda, Effective replacement of cetyltrimethylammonium bromide (CTAB) by mercaptoalkanoic acids on gold nanorod (AuNR) surfaces in aqueous solutions, Nanoscale 12 (2020) 658–668.
[18] C.J. Murphy, L.B. Thompson, A.L. Alkilany, P.N. Sisco, S.P. Boulos, S.T. Sivapalan, J.A. Yang, D.J. Chernak, J. Huang, The many faces of gold nanorods, J. Phys. Chem. Lett. 1 (2010) 2867–2875.
[19] L. Shao, H. Chen, Q. Li, J. Wang, Gold nanorods and their plasmonic properties, Chem. Soc. Rev. 42 (2012) 2679.
[20] D. Nepal, K. Park, R.A. Vaia, High-yield assembly of soluble and stable gold nanorod pairs for high-temperature plasmonics, Small 8 (2012) 1010–1020.
[21] J.M. Gisbert-González, M.V. Oliver-Pardo, V. Briega-Martos, J.M. Feliu, E. Herrero, Charge effects on the behavior of CTAB adsorbed on Au(111) electrodes in aqueous solutions, Electrochim. Acta (2021) 370.
[22] J. Clavilier, R. Faure, G. Guinet, R. Durand, Preparation of monocrystalline Pt microelectrodes and electrochemical study of the plane surfaces cut in the direction of the {111} and {110} planes, J. Electroanal. Chem. 107 (1980) 205–209.
[23] A. Rodes, E. Herrero, J.M. Feliu, A. Aldaz, Structure sensitivity of irreversibly adsorbed tin on gold single-crystal electrodes in acid media, J. Chem. Soc. Faraday T. 92 (1996) 3769–3776.
[24] V. Climent, B.A. Coles, R.G. Compton, Coulostatic potential transients induced by laser heating of a Pt(111) single-crystal electrode in aqueous acid solutions. rate of hydrogen asorption and potential of maximum entropy, J. Phys. Chem. B 106 (2002) 5988–5996.
[25] V. Climent, B.A. Coles, R.G. Compton, Laser-induced potential transients on a Au(111) single-crystal electrode. Determination of the potential of maximum entropy of double layer formation, J. Phys. Chem. B 106 (2002) 5258–5265.
[26] S. Narasimhan, D. Vanderbilt, Elastic stress domains and the herringbone reconstruction on Au(111), Phys. Rev. Lett. 69 (1992) 1564–1567.
[27] U. Harten, A.M. Lahee, J.P. Toennies, C. Wöll, Observation of a soliton reconstruction of au(111) by high-resolution helium-atom diffraction, Phys. Rev. Lett. 54 (1985) 2619–2622.
[28] R.J. Needs, M. Mansfield, Calculations of the surface stress tensor and surface energy of the (111) surfaces of iridium, platinum and gold, J. Phys. 1 (1989) 7555–7563.
[29] A. Sadkowski, A.J. Motheo, R.S. Neves, Characterisation of au(111) and au(210) aqueous solution interfaces by electrochemical immittance spectroscopy, J. Electroanal. Chem. 455 (1998) 107–119.
[30] U.W. Hamm, D. Kramer, R.S. Zhai, D.M. Kolb, The pzc of Au(111) and Pt(111) in a perchloric acid solution: an ex situ approach to the immersion technique, J. Electroanal. Chem. 414 (1996) 85–89.
[31] A. Hamelin, Cyclic voltammetry at gold single-crystal surfaces .1. Behaviour at low-index faces, J. Electroanal. Chem. 407 (1996) 1–11.
[32] X. Gao, S.C. Chang, X. Jiang, A. Hamelin, M.J. Weaver, Emergence of atomic level structural information for oredered metal-solution interfaces : some recent contributions from in- situ infrared spectroscopy and scanning tunneling microscopy, J. Vac. Sci. Technol. A 10 (1992) 2972.
[33] A. Hamelin, L. Stoicoviciu, G.J. Edens, X. Gao, M.J. Weaver, Some electrochemical consequences of potencial-induced surface reconstruction on Au(100): double layer nonuniformity and electrode kinetics, J. Electroanal. Chem. 365 (1994) 47–57.
[34] A.N. Frumkin, O.A. Petrii, B.B. Damaskin, Potential of Zero Charge, in: J.O. Bockris, B.E. Conway, E. Yeager (Eds.) Comprehensive Treatise of Electrochemistry, Plenum, New York, 1980, pp. 221-289.
[35] C.L. Brosseau, E. Sheepwash, I.J. Burgess, E. Cholewa, S.G. Roscoe, J. Lipkowski, Adsorption of N-Decyl-N,N,N-trimethylammonium Triflate (DeTATf), a cationic surfactant, on the Au(111) electrode surface, Langmuir 23 (2007) 1784–1791.
[36] M.A. Van Hove, R.J. Koestner, P.C. Stair, J.P. Biberian, L.L. Kesmodel, I. Bartos, G.A. Somorjai, The surface reconstructions of the (100) Crystal Faces of Iridium, Platinum, and Gold: I. Experimental observations and possible structural models, Surf. Sci. 103 (1981) 189–217.
[37] D.M. Kolb, J. Schneider, Surface reconstuction in electrochemistry: Au(100)-(5×20), Au(111)-(1×23) and Au(110)-(1×2), Electrochim. Acta 31 (1986) 929–936.
[38] X. Gao, A. Hamelin, J.M. Weaver, Potential-dependent reconstruction at ordered Au(100)-aqueous interfaces as probed by atomic-resolution scanning tunneling microscopy, Phys. Rev. Lett. 67 (1991) 618–621.
[39] X. Gao, A. Hamelin, M.J. Weaver, Elucidating complex surface reconstruction with atomic resolution scanning tunneling microscopy: Au(100) aqueous electrochemical interface, Phys. Rev. B 46 (1992) 7096–7102.
[40] G. Binnig, H. Rohrer, G. Ch, E. Weibel, (111) facets as the origin of reconstructed Au(110) surfaces, Surf. Sci. Lett. 131 (1983) L379-L384.
[41] X. Gao, A. hamelin, J.M. Weaver, Reconstruction at ordered Au(110)-aqueous interfaces as probed by atomic-resolution scanning tunneling microscopy, Phys. Rev. B - Condens. Matter Mater. Phys. 44 (1991) 10983–10986.
[42] A. Hamelin, M.J. Weaver, Dependence of the kinetics of proton reduction at gold electrodes on the surface cyrstallographic orientation, J. Electroanal. Chem. Interfac. Electrochem. 223 (1987) 171–184.
[43] J.P. Vivek, I.J. Burgess, Quaternary ammonium bromide surfactant adsorption on low-index surfaces of gold. 1. Au(111), Langmuir 28 (2012) 5031–5039.
[44] J.P. Vivek, I.J. Burgess, Quaternary ammonium bromide surfactant adsorption on low-index surfaces of gold. 2. Au(100) and the role of crystallographic-dependent adsorption in the formation of anisotropic nanoparticles, Langmuir 28 (2012) 5040–5047.
[45] J.P. Vivek, I.J. Burgess, Adsorption of a quaternary ammonium surfactant on Au(100), J. Electroanal. Chem. 649 (2010) 16–22.